MATERIALS

Sediment samples

In this study, we have analyzed three sediment cores from the Japan Sea obtained by Integrated Ocean Drilling Program (IODP) Expedition 346 (Tada et al., 2015) and from the Deep Sea Drilling Project (DSDP) site 296 in the western North Pacific (Ingle et al., 1975). We have mainly analyzed Nd isotopes of fossil fish teeth/debris (FT/FD) from core U1425 at the Yamato Rise in the central part of the Japan Sea and DSDP 296 for the last 10 Ma, and have also analyzed Nd isotopes of fossil FT/FD from only Holocene sediments at site U1426 and site U1430 in the Japan Sea (Fig. 1). Detailed information on sediment cores analyzed in this study are given in Table DR1.

Sediments obtained from site U1425 are composed mainly of quartz, plagioclase, and clay minerals (Tada et al., 2015). There is a major contribution of biogenic opal and detrital clay/silt, and calcium carbonate content is generally low throughout the core (Tada et al., 2015). The lithostratigraphic Unit I is composed of light-dark alternate layers, reflecting oscillations in deep-water oxic–anoxic conditions due to cyclic activation of deep-water formation in the Japan Sea from 2.6–2.5 Ma (Tada, 1994; Tada et al., 2015) (Fig. DR4). Unit II is characterized by the diatomaceous clay and diatom ooze. Sub-unit IIB has relatively lower bulk densities, representing higher diatom contents compared with sub-unit IIA (Tada et al., 2015). The distinct ε_{Nd} shift observed at 4.5 Ma was almost coincident with the IIA/IIB unit boundary, suggesting that the onset of the ε_{Nd} shift is related to gradual increases in terrigenous material fluxes and/or decreases in diatom burial fluxes (Fig. DR4).

The initial age model for core U1425 was originally based on datums of paleomagnetism, tephra, radiolarians, diatoms, planktonic foraminifers, and calcareous nannofossils, which were determined from an on-board study (Tada et al., 2015). In this paper, we have used the combined age–depth model, which applies on-board paleomagnetic datums and recently updated radiolarian datums (Kamikuri et al., 2017) (Fig. DR1 and Table DR2). The age–depth plot of core U1425 was produced by assuming linear sedimentation rates between the age control points (Fig. DR1). If we used the on-board age–depth relationship, the age differences with the age model used in this study are less than 0.3 Myr for the interval 4 to 5 Ma. The choice of the age models does not significantly affect the conclusions of this study. For DSDP 296, we used the published age model based on planktonic foraminifers (Ujiie, 1975).

For FT/FD and Fe-Mn oxide leachate, we sampled U1425 at various sampling intervals (0.06–18.8 m) throughout the core (n = 69). Sample density increased around 4.5 Ma, and the average stratigraphic resolution for Nd isotope records was 0.14 Myr for the past 10 Ma. The stratigraphic resolution of Nd isotope data (n = 26) for DSDP296 was 0.4 Ma. For the detrital fraction for core U1425, we selected 18 samples for the past 10 Ma.

Seawater samples

Unfiltered seawater samples were collected onboard R/V Hakuho-Maru from July 15, 1998 to August 14, 1998 (KH-98-3). Approximately 300 L of surface seawaters were collected via built-in pump system (~5 m below sea level), and transferred to a plastic container on the ship (Amakawa at al., 2004a). Except for the surface samples, the samples (20 L for station CM-19 and 250 L for station CM-20) were collected with a large volume water sampler (N12-1000, Nichiyu-Giken Kogyo Co. Ltd.). After sampling, all the samples were acidified to pH < 2 using HCl. The procedure of subsequent chemical separation of Nd was identical to that detailed in Amakawa *et al.* (2004b).

METHODS

Preparation of FT/FD, Fe-Mn oxide leachate, and residues

FT/FD were cleaned using ultrasonication in ultrapure water and methanol (Super Special

Grade from Wako Pure Chemical Industries, Ltd., Osaka, Japan) three times to remove sediment particles absorbed on them (Horikawa et al., 2011). Then, after the samples were rinsed by ultrapure water three times, samples were completely dissolved in an admixture (1:1) of ultrapure concentrated HNO_3 and HCl (TAMAPURE-AA-100 from Tama Chemicals, Ltd., Tokyo, Japan) by refluxing for more than 2 hours at 80°C. Sample solutions were evaporated (130°C), and re-dissolved with 1.8 M HCl.

To measure Nd isotopes of Fe-Mn oxide leachate of bulk sediments from core U1425, we leached bulk sediments (~1.0 g) according to sequential leaching methods (Bayon et al., 2002; Piotrowski et al., 2004). First, carbonate in the sediment samples was dissolved via treatment for two hours at room temperature in 10% buffered acetic acid (decarbonation). The samples were rinsed by ultrapure water three times. Then, the Fe-Mn oxide fraction was leached using 0.02 M hydroxylamine hydrochloride (HH) in 25% acetic acid (Ultrapur from Kanto Chemical Co., INC., Tokyo, Japan) for two hours at room temperature. The leached Fe-Mn fraction was dried, and re-dissolved using 1.8 M HCl for chemical separation as for FT/FD samples.

The residue samples were prepared from after removing carbonate, oxide and biogenic silica fractions in the sediments. Biogenic silica fraction was leached for 30 min with 1M NaOH (Ultrapur from Kanto Chemical Co., INC., Tokyo, Japan) at a temperature of 80°C. After drying the residues, the residues were weighted (40–60 mg) and completely digested by an admixture of concentrated HNO_3, HCl, and HF (TAMAPURE-AA-100 from Tama Chemicals, Ltd., Tokyo, Japan) by refluxing for more than 12 hours at 130°C. The residue fraction was dried, and re-dissolved using 1.8 M HCl for chemical separation as for FT/FD samples.

Chemical separation for Nd and Nd isotope analysis

Chemical separation for Nd was carried out as follows: (1) Major elements were removed from sample solution by using a cation exchange resin column (MCI GEL CK08P, Mitsubishi Chemical Corporation) with 1.8 M HCl, (2) The REE fraction was extracted using 4.5 M HCl eluent, (3) The Nd fraction was isolated from REEs by using a Ln-spec resin column (50–100 μm, Eichrom Technologies) with 0.25 M HCl eluent. All reagents used in this procedure were trace metal grade reagents (TAMAPURE-AA-100 from Tama Chemicals, Ltd., Tokyo, Japan) and all procedures were done in a clean laboratory at the University of Toyama.

Nd isotopic compositions of FT/FD, Fe-Mn oxide leachates, and residues were measured with a thermal ionization mass spectrometer (TIMS) (IsoProbe-T, GVI) at Nagoya University. Nd isotopes were measured as Nd^+ using a Re triple filament assembly for samples with a large amount of Nd (> 35 ng) and as NdO^+ using a single W filament with a Ta-emitter (Chu et al., 2009, 2014) for samples with lower amounts of Nd (5–20 ng Nd). Measured Nd isotope ratios ($^{143}Nd/^{144}Nd$) were corrected for mass fractionation using $^{146}Nd/^{144}Nd = 0.7219$. The average of Nd isotope ratios of international standard JNdi-1 was 0.512115 ± 0.000008 (2σ, n = 27) during the study period, which was in good agreement with the recommended value (0.512115 ± 0.000007) (Tanaka et al., 2000). Since the Nd isotope ratio measured as Nd^+ was in good agreement with the recommended value, we determined that there was no necessity to correct values using the data of JNdi-1. The data of JNdi-1 measured as NdO^+ was varied according as the amount of Nd. Therefore, the sample data measured as NdO^+ were corrected by the JNdi-1 data that were measured using similar beam intensity.

Nd isotopic compositions of seawater were measured as Nd^+ with a TIMS (Finnigan MAT262) at The University of Tokyo using a Re double filament assembly. The measured seawater data were corrected along with the measured JNdi-1 standard or La Jolla standard values, adjusting to the recommended values (JNdi-1 standard = 0.512115 (Tanaka et al., 2000); La Jolla standard = 0.511858 (Lugmair et al., 1983)).

All Nd isotope data used in this study are given in Tables DR3 and DR4.

CONSISTENCY OF ε_{Nd} VALUES FOR FT/FD AND Fe-Mn OXIDE LEACHATE

Nd isotopic compositions of authigenic sedimentary archives, such as fossil FT/FD and early diagenetic ferromanganese coatings of bulk sediments and planktonic foraminifera, represent bottom water ε_{Nd}, and thus are widely used in reconstructing water mass provenances and/or mixing (i.e., circulation) in the past (Frank, 2002). In this study, we mainly applied fossil FT/FD for extracting bottom water ε_{Nd} to avoid volcanic debris contamination problems associated with bulk sediment leachate analysis (Horikawa et al., 2011; Roberts et al., 2010; Wilson et al., 2013). However, low yields of fossil FT/FD due to higher opal fluxes limited the generation of the continuous ε_{Nd} record from U1425, especially for the period 6–4 Ma (Fig. 2). To compensate for the lack of FT/FD ε_{Nd} for this period, we used Nd isotopic compositions of Fe-Mn oxide leachate.

It is known that Fe-Mn oxide leaching of decarbonated sediments causes a deviation of ε_{Nd} from seawater ε_{Nd} due to contamination with Nd deriving from lithogenic particles (Wu et al., 2015). Caution should therefore be exercised in the use of such leaching procedures. In our data set, leaching of the Fe-Mn oxide from decarbonated sediments showed a good consistency with FT/FD ε_{Nd} values, although some samples of leachate present a slight offset towards less radiogenic ε_{Nd} values (~0.5 ε_{Nd} unit) compared to FT/FD ε_{Nd} (Fig. DR2 and Table DR3). Based on this evaluation, we concluded the ε_{Nd} data from Fe-Mn oxide leachate can be used as the comparable data to actual bottom water ε_{Nd} for the period 6–4 Ma (Fig. 2).

OCEANOGRAPHY RELATED Nd ISOTOPE COMPOSITIONS

TWC is the dominant surface current (2.65 Sv, 1 Sv = 10^6 m^3/s, Fukudome et al., 2010) in the Japan Sea, whereas freshwater input from the Japanese Islands (0.0034 Sv) and the Liman Current (0.0026 Sv) are negligible (Japan River Association, 2002; Lee and Nam, 2004) (Fig. 1). TWC is the admixed water of Changjiang diluted water (–11.1 ± 0.3 ε_{Nd}), Kuroshio Water (–3.4 ± 0.6 ε_{Nd}), and Yellow Sea Water (–14.3 ± 0.3 ε_{Nd}) (Che and Zhang, 2018), and might be influenced by potential weathering inputs of Nd from very old rocks in South Korea (river sediments of −19.7 ε_{Nd}) (Lan et al., 1995). As a result, the surface water in the Japan Sea attains lower radiogenic values of around –8 ε_{Nd} (Amakawa et al., 2004a).

The deep water in the Japan Sea, called Japan Sea Proper Water (JSPW), is formed off the Russian coast during extremely cold winters in association with cold winter monsoons. A rapid turnover time (~100 yr) of the bottom water creates a homogeneous deep-water mass with an extremely narrow range in water temperatures (0.0–0.2 °C) and salinities (34.06–34.07) (Gamo et al., 1986; Kumamoto et al., 1998) (Fig. DR3). These observations also account for the homogeneous deep-water ε_{Nd} value of –6.84 ± 0.4 (> 400 m water depth, n = 14, 2σ) in the Japan Sea (Fig. 2 and Table DR4).

Given that the deep-water ε_{Nd} value is slightly more radiogenic than that of TWC and that the source area of JSPW is off the Russian coast, Liman Current flowing along the northern Japan Sea is likely to have supplied radiogenic Nd. This is supported by the evidence that detrital ε_{Nd} values at DSDP 301 (41°03.75'N, 134°02.86'E) in the northern Japan Sea represented radiogenic values (–4.9 to –8.8 ε_{Nd} for 1.4–2.3 Ma) at some intervals (Mahoney, 2005).

The ε_{Nd} values of Holocene FT/FD and oxide leachate at site U1430 and site U1425 present a light offset from the average ε_{Nd} value (–6.84 ± 0.4 ε_{Nd}) of the deep seawater in the Japan Sea (CM-19 and CM-20) (Fig. 2). The FT/FD ε_{Nd} value (–7.68 ε_{Nd}) at site U1430 presents a slightly less radiogenic value compared to the seawater ε_{Nd}, which might be affected by boundary exchange with Nd of lithogenic particles deriving from Korean Peninsula. In contrast, the reason for the slight difference observed at site U1425 has not yet been

determined. Assuming that the deep-water in the Japan Sea represents the homogeneous Nd isotopic composition, the preferred explanation for the slight offset is boundary exchange at the Yamato Rise. At this point, although core-top ε_{Nd} values of detrital materials in the Japan Sea are not available, ε_{Nd} values of detrital fractions ranged from –4.9 to –8.8 ε_{Nd} for 1.4–2.3 Ma at DSDP 301 (41°03.75'N, 134°02.86'E) in the northern Japan Sea. From currently available data, we consider exchange of radiogenic material in sediments with bottom water at the Yamato Rise as a potential cause for the slight offset.

REFERENCES CITED

Amakawa, H., Alibo, D.S., and Nozaki, Y., 2004a, Nd concentration and isotopic composition distributions in surface waters of Northwest Pacific Ocean and its adjacent seas pages paires: Geochemical Journal, v. 38, p. 493–504, doi:10.2343/geochemj.38.493.

Amakawa, H., Nozaki, Y., Alibo, D.S., Zhang, J., Fukugawa, K., and Nagai, H., 2004b, Neodymium isotopic variations in Northwest Pacific waters: Geochimica et Cosmochimica Acta, v. 68, p. 715–727, doi:10.1016/S0016-7037(03)00501-5.

Bayon, G., German, C.R., Boella, R.M., Milton, J.A., Taylor, R.N., and Nesbitt, R.W., 2002, An improved method for extracting marine sediment fractions and its application to Sr and Nd isotopic analysis: Chemical Geology, v. 187, p. 179–199, doi:10.1016/S0009-2541(01)00416-8.

Che, H., and J. Zhang, 2018, Water mass analysis and end-member mixing contribution using coupled radiogenic Nd isotopes and Nd concentrations: Interaction between marginal seas and the Northwestern Pacific: Geophysical Research Letters, v. 45, p. 2388–2395, doi:10.1002/2017GL076978.

Chu, Z., Chen, F., Yang, Y., and Guo, J., 2009, Precise determination of Sm, Nd concentrations and Nd isotopic compositions at the nanogram level in geological samples by thermal ionization mass spectrometry: Journal of Analytical Atomic Spectrometry, v. 24, p. 1534–1544, doi:10.1039/b904047a.

Chu, Z., Guo, J., Yang, Y., Qi, L., and Li, C., 2014, Precise determination of Sm and Nd concentrations and Nd isotopic compositions in highly depleted ultramafic reference materials: Geostandards and Geoanalytical Research, v. 38, p. 61–72, doi:10.1111/j.1751-908X.2013.00224.x.

Frank, M., 2002, Radiogenic Isotopes: Tracers of past ocean circulation and erosional input: Reviews of Geophysics, v. 40, p. 1-1−1-38, doi:10.1029/2000RG000094.

Fukudome, K., Yoon, J.H., Ostrovskii, A., Takikawa, T., and Han, I.S., 2010, Seasonal volume transport variation in the Tsushima Warm current through the Tsushima Straits from 10 years of ADCP observations: Journal of Oceanography, v. 66, p. 539–551, doi:10.1007/s10872-010-0045-5.

Gamo, T., Nozaki, Y., Sakai, H., Nakai, T., and Tsubota, H., 1986, Spacial and temporal variations of water characteristics in the Japan Sea bottom layer: Journal of Marine Research, v. 44, p. 781–793, doi:10.1357/002224086788401620.

Horikawa, K., Martin, E.E., Asahara, Y., and Sagawa, T., 2011, Limits on conservative behavior of Nd isotopes in seawater assessed from analysis of fish teeth from Pacific core tops: Earth and Planetary Science Letters, v. 310, p. 119–130, doi:10.1016/j.epsl.2011.07.018.

Ingle, J.C. et al., 1975, Site 296. In Initial Reports of the Deep Sea Drilling Project, 31: U.S. Government Printing Office, doi:10.2973/dsdp.proc.31.107.1975.

Japan River Association, 2002, Rivers in Japan: http://www.japanriver.or.jp/river_law/map.htm (accessed April 2018).

Kamikuri, S., Itaki, T., Motoyama, I., and Matsuzaki, M.K., 2017, Radiolarian biostratigraphy from middle Miocene to late Pleistocene in the Japan Sea: Paleontological Research, v. 21, p. 397–421, doi:10.2517/2015PR015.

Kumamoto, Y., Yoneda, M., Shibata, Y., Kume, H., Tanaka, A., Uehiro, T., Morita, M., and Shitashima, K., 1998, Direct observation of the rapid turnover of the Japan Sea bottom water by means of AMS radiocarbon measurement: Geophysical Research Letters, v. 25, p. 651–654, doi:10.1029/98GL00359.

Lan, C.Y., Lee, T., Zhou, X.H. and Kwon, S.T., 1995, Nd isotopic study of Precambrian

basement of South Korea: evidence for early Archean crust?: Geology, v. 23, p. 249–252, doi:10.1130/0091-7613(1995)023<0249:NISOPB>2.3.CO;2.

Lee, E., and Nam, S., 2004, Low sea surface salinity in the East Sea during the last glacial maximum: Review on freshwater supply: Geosciences Journal, v. 8, p. 43–49, doi:10.1007/BF02910277.

Lugmair, G.W., Shimamura, T., Lewis, R.S., and Anders, E., 1983, Samarium–146 in the early solar system: evidence from neodymium in the Allende meteorite: Science, v. 222, p. 1015–1018.

Mahoney, J. B., 2005, Nd and Sr isotopic signatures of fine-grained clastic sediments: A case study of western Pacific marginal basins: Sedimentary Geology, v. 182, p. 183–199, doi:10.1016/j.sedgeo.2005.07.009.

Piepgras, D.J., and Jacobsen, S.B., 1988, The isotopic composition of neodymium in the North Pacific: Geochimica et Cosmochimica Acta, v. 52, p. 1373–1381, doi:10.1016/0016-7037(88)90208-6.

Piotrowski, A.M., Goldstein, S.L., Hemming, S.R., and Fairbanks, R.G., 2004, Intensification and variability of ocean thermohaline circulation through the last deglaciation: Earth and Planetary Science Letters, v. 225, p. 205–220, doi:10.1016/j.epsl.2004.06.002.

Reid, J.L., 1994, On the total geostrophic circulation of the North Atlantic Ocean: Progress in Oceanography, v. 33, p. 1–92, https://doi.org/10.1016/0079-6611(94)90014-0.

Roberts, N.L., Piotrowski, A.M., McManus, J.F., and Keigwin, L.D., 2010, Synchronous deglacial overturning and water mass source changes: Science, v. 327, p. 75–78, doi:10.1126/science.1178068.

Tada, R., 1994, Paleoceanographic evolution of the Japan Sea: Palaeogeography, Palaeoclimatology, Palaeoecology, v. 108, p. 487–508, doi:10.1016/0031-0182(94)90248-8.

Tada, R. et al., 2015, Proceedings of Integrated Ocean Drilling Program, volume 346, College Station, TX (Integrated Ocean Drilling Program). doi:10.2204/iodp.proc.346.101.2015.

Tanaka, T. et al., 2000, JNdi-1: A neodymium isotopic reference in consistency with La Jolla neodymium: Chemical Geology, v. 168, p. 279–281, doi:10.1016/S0009-2541(00)00198-4.

Ujiie, H., 1975, 35. Planktonic foraminiferal biostratigraphy in the western Philippine Sea, Leg 31 of DSDP: Deep Sea Drilling Project Initial Reports, v. 31, p. 677–691, doi:10.2973/dsdp.proc.31.135.1975.

van de Flierdt, T., Martin, F., Lee, D.C., Halliday, A.N., Reynolds, B.C., and Hein, J.R., 2004, New constraints on the sources and behavior of neodymium and hafnium in seawater from Pacific Ocean ferromanganese crusts: Geochimica et Cosmochimica Acta, v. 68, p. 3827–3843, doi:10.1016/j.gca.2004.03.009.

van de Flierdt, T., Martin, F., Halliday, A.N., Hein, J.R., Hattendorf, B., Günther, D., and Kubik, P.W., 2003, Lead isotopes in North Pacific deep water - implications for past changes in input sources and circulation patterns: Earth and Planetary Science Letters, v. 209, p.149–164, doi:10.1016/S0012-821X(03)00069-4.

Whitworth, T., Orsi, A.H., Kim, S.-J., Nowlin Jr., W.D., and Locarnini, R.A., 1998, Water masses and mixing near the Antarctic slope front: Ocean, Ice and Atmosphere: Interactions at the Antarctic Continental Margin, v. 75, p. 1–27, doi:10.1029/AR075p0001.

Wilson, D.J., Piotrowski, A.M., Galy, A., and Clegg, J.A., 2013, Reactivity of neodymium carriers in deep sea sediments: Implications for boundary exchange and paleoceanography: Geochimica et Cosmochimica Acta, v. 109, p. 197–221, doi:10.1016/j.gca.2013.01.042.

Wu, Q., Colin, C., Liu, Z., Thil, F., Dubois-Dauphin, Q., Frank, N., Tachikawa, K., Bordier, L., and Douville, E., 2015, Neodymium isotopic composition in foraminifera and authigenic phases of the South China Sea sediments: Implications for the hydrology of the North Pacific Ocean over the past 25 kyr: Geochemistry, Geophysics, Geosystems, v. 16, p. 3883–3904, doi:10.1002/2015GC005871.

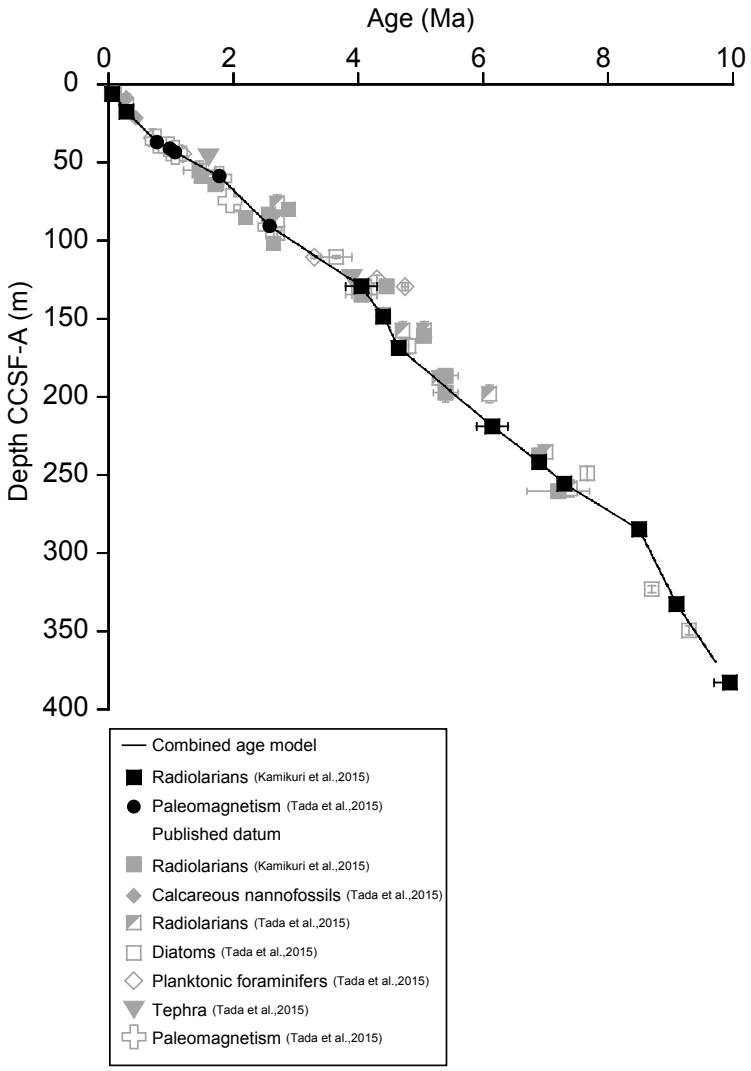

Figure DR1. Age–depth relationship for IODP U1425D. We used the combined age–depth relationship which applies on-board paleomagnetic datums (black circles, Tada et al., 2015) and recently updated radiolarian datums (black squares, Kamikuri et al., 2017). The age control datums used in this study are given in Table DR2.

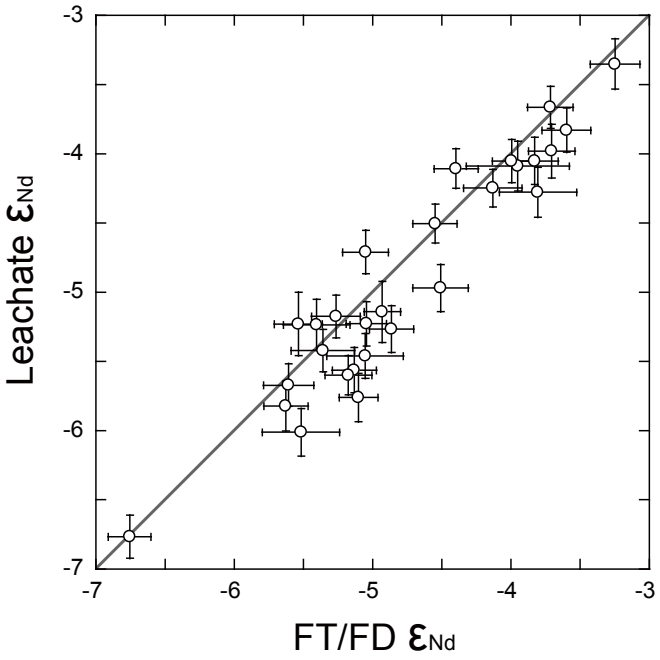

Figure DR2. Comparison of Nd isotopic composition (ε_{Nd}) of FT/FD and Fe-Mn oxide leachate from IODP site U1425. The data of Fe-Mn oxide are in good agreement with FT/FD ε_{Nd}. The error bars show the 2SE (internal error). The data is given in Table DR3.

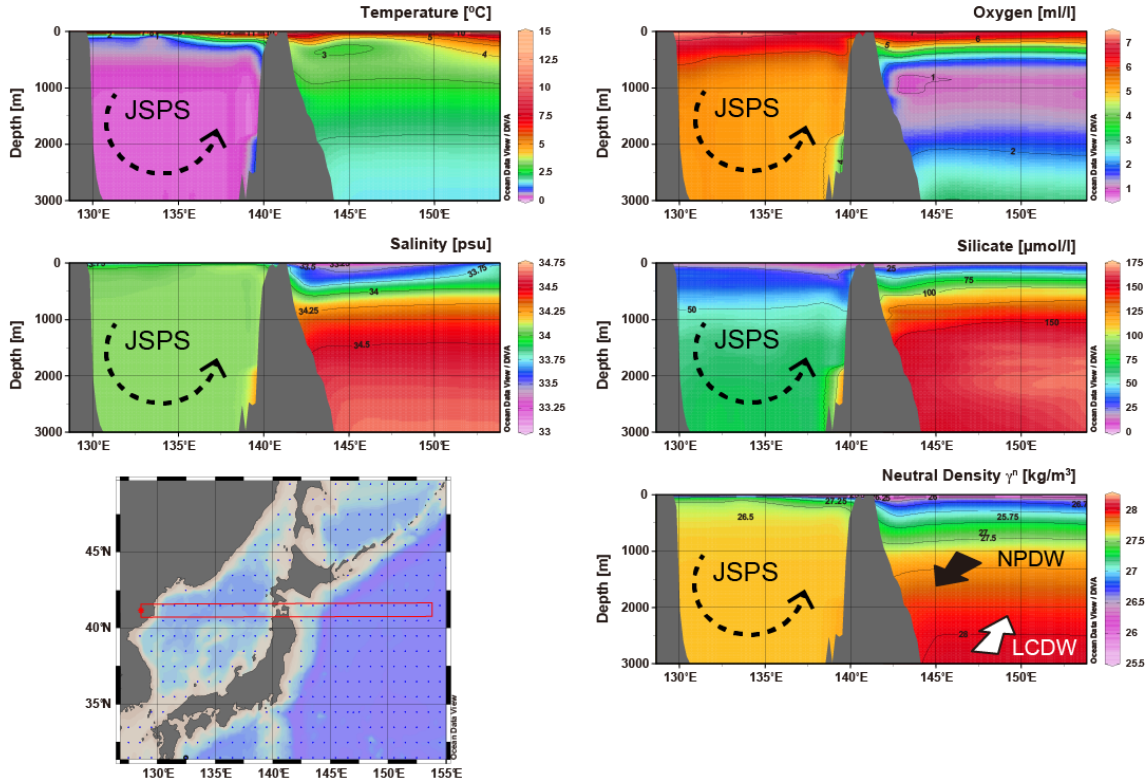

Figure DR3. East–West section across Northern Japan Arc (red box on section), showing temperature (ºC), salinity (PSU), oxygen concentrations (ml/l), silicate concentrations (µmol/l), and neutral density (kg/m^3) in the Japan Sea and the North Pacific. Unlike the North Pacific, the deep water in the Japan Sea, called Japan Sea Proper Water (JSPW), represents a homogenous water mass (oxygen and silicate) with an extremely narrow range in water temperatures (0.0–0.2 °C) and salinities (34.06–34.07). Deep waters in the western North Pacific consist of Lower Circumpolar Deep Water (LCDW) and North Pacific Deep Water (NPDW). LCDW is an advected flow from the Southern Ocean, and NPDW is the return flow of LCDW upwelled in the North Pacific (Reid, 1994). The LCDW is defined by a neutral density range of 28.00 kg/m^3 $<\gamma^n<$28.27 kg/m^3 (Whitworth et al., 1998). All seawater data are from the database of the World Ocean Atlas 13. Map was produced using Ocean Data View (Schlitzer, R., 2011, http://odv.awi.de.).

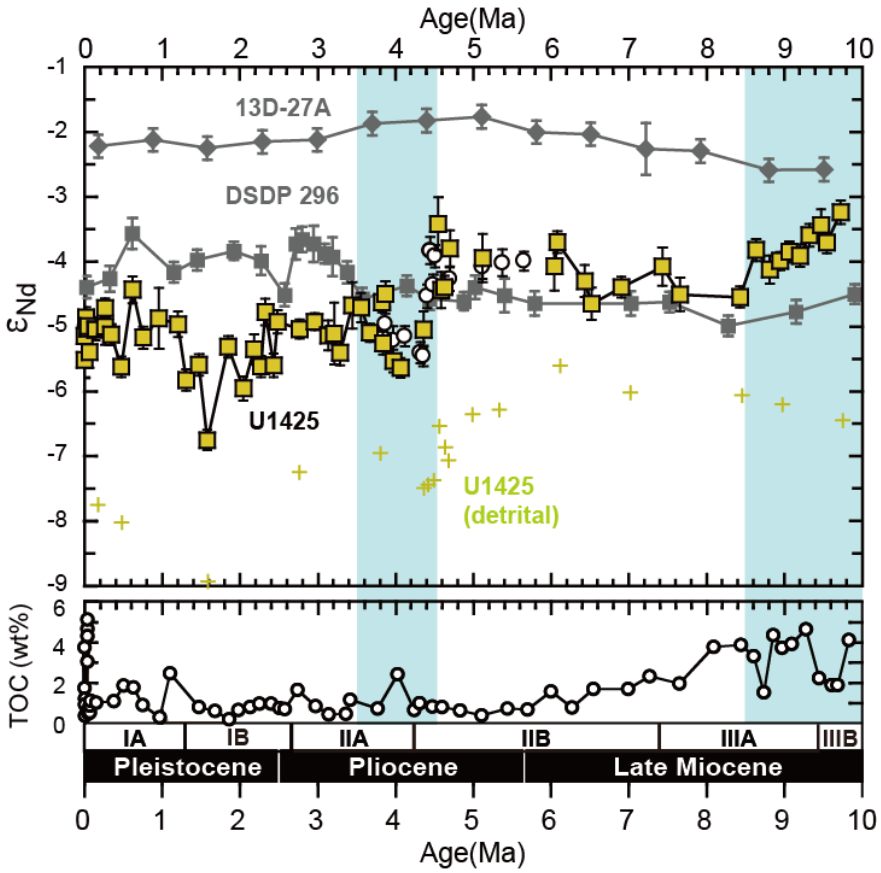

Figure DR4. Nd isotope records from IODP U1425 in the Japan Sea, DSDP 296 in the western subtropical Pacific, 13D-27A in the western North Pacific (see the main text). Detrital ε_{Nd} values are also shown. Bottom panel shows total organic carbon (TOC) from core U1425 (Tada et al., 2015). The ongoing declines in TOC (wt%) represent gradually decreased inflow of nutrient-enriched Oyashio/NPDW into the Japan Sea from ~9 Ma.

TABLE DR1. LIST OF SAMPLES

Area	Cruise	Site	Latitude (N)	Longitude (E)	Water Depth (m)	Sample type	Reference	Age model	Reference of age model
Japan Sea	IODP Exp.346	U1425D	39°29.4392′	134°26.5395′	1909	FT/FD	This study	Magnestratigraphy and Biostratigraphy (radiolarian)	Kamikuri et al. (2017) and Tada et al. (2015)
Japan Sea	IODP Exp.346	U1426A	37°1.9996′	134°47.9999′	903	FT/FD	This study	Magnestratigraphy	Tada et al. (2015)
Japan Sea	IODP Exp.346	U1430A	37°54.1595′	131°32.2499′	1072	FT/FD	This study	Magnestratigraphy	Tada et al. (2015)
Western North Pacific	DSDP	296	29°20.41′	133°31.52′	2909	FT/FD	This study	Biostratigraphy (planktonic foraminifera)	Ujiie (1975)
Western North Pacific	RNDB06	13D-27A	51°27.8′	167°38.2′	1500−1800	crust	van de Flierdt et al. (2004)	$^{10}Be/^{9}Be$	van de Flierdt et al. (2003)
Japan Sea	KH-98-3	CM-19	41°21′	137°20′	3557	Seawater	This study	—	—
Japan Sea	KH-98-3	CM-20	37°44′	135°14′	2727	Seawater	This study	—	—
Western North Pacific	TPS47	39-1	47°00.0′	161°08.2′	5408	Seawater	Piepgras and Jacobsen (1988)	—	—
Western North Pacific	KH-94-3	LM-2	29°05′	142°51′	9017	Seawater	Amakawa et al. (2004b)	—	—

TABLE DR2. AGE MODEL FOR CORE U1425

Datum	Depth (m, CCSF-A)	Age (Ma)	Age control point (Ma)
Top	0		0
LO Lychnocanoma sakaii†	6.08	0.054	0.054
LO Schizodiscus japonicus†	17.58	0.29	0.29
Bottom of C1n (Brunhes/Matuyama)*	37.27	0.781	0.781
Top of C1r.1n (Jaramillo)*	41.57	0.988	0.988
Bottom of C1r.1n (Jaramillo)*	43.57	1.072	1.072
Top of C2n (Olduvai)*	59.09	1.778	1.778
Top of C2An.1n (Matuyama/Gauss)*	90.76	2.581	2.581
FO Hexacontium parviakitaense†	129.385	3.8-4.3	4.05
FO Dictyophimus bullatus†	148.51	4.3-4.5	4.4
RI Siphocampe arachnea group†	168.51	4.6-4.7	4.65
LO Lychnocanoma parallelipes†	219.00	5.9-6.4	6.15
FO Axoprunum acquilonium†	241.805	6.8-7.0	6.9
FO Lychnocanoma parallelipes†	255.58	7.2-7.4	7.3
FO Cycladophora sphaeris†	284.855	8.5	8.5
LO Lychnocanoma magnacornuta†	332.68	9.1	9.1
FO Cycladophora nakasekoi†	382.925	9.7-10.2	9.95

*Tada et al. (2015)

†Kamikuri et al. (2017)

TABLE DR3. Nd ISOTOPIC COMPOSITIONS OF U1425 AND DSDP 296

Cruise	Site	Section	Section depth (cm) Top	Section depth (cm) Bottom	Mid depth (CCSF-A, m)	Age (Ma)	$^{143}Nd/^{144}Nd$ FT/FD	± 2SE	$\varepsilon_{Nd}(0)$	2SE	$^{143}Nd/^{144}Nd$ Fe-Mn oxide	± 2SE	$\varepsilon_{Nd}(0)$	2SE	$^{143}Nd/^{144}Nd$ Detrital	± 2SE	$\varepsilon_{Nd}(0)$	2SE
IODP Exp.346	**U1426A**				0.346	0.0031	0.512301	± 20	-6.57	0.40								
IODP Exp.346	**U1430A**				0.240	0.0053	0.512244	± 25	-7.68	0.50								
IODP Exp.346	**U1425D**	1H-1	4	6	0.050	0.0008	0.512355	± 14	-5.52	0.28	0.512330	± 9	-6.01	0.17				
		1H-1	31	37	0.340	0.0056	0.512374	± 8	-5.15	0.16								
		1H-2	59	61	2.100	0.0346	0.512389	± 8	-4.86	0.16	0.512368	± 9	-5.27	0.17				
		1H-3	103	105	4.040	0.0666	0.512380	± 9	-5.04	0.18								
		1H-CC	0	3	5.015	0.0827	0.512382	± 11	-5.00	0.22								
		2H-1	3	5	6.405	0.1057	0.512361	± 12	-5.40	0.24	0.512370	± 9	-5.23	0.18				
		2H-3	102	104	10.095	0.1665	0.512379	± 8	-5.05	0.17	0.512397	± 8	-4.71	0.16	0.512241	± 8	-7.74	0.16
		3H-1	82	88	16.442	0.2712	0.512381	± 14	-5.01	0.28								
		3H-1	90	92	16.502	0.2722	0.512396	± 8	-4.72	0.15								
		3H-3	103	105	19.632	0.3412	0.512375	± 8	-5.13	0.16	0.512353	± 8	-5.56	0.16				
		3H-CC	0	3	24.957	0.4740	0.512350	± 8	-5.63	0.16	0.512340	± 9	-5.82	0.18	0.512228	± 8	-8.01	0.16
		4H-3	102	104	30.758	0.6186	0.512410	± 10	-4.44	0.21								
		4H-CC	0	3	36.253	0.7556	0.512373	± 9	-5.18	0.17	0.512351	± 7	-5.60	0.14				

5H-3	102	104	40.896	0.9555	0.512388	±	24	-4.88	0.47										
5H-CC	0	2	46.376	1.1996	0.512383	±	10	-4.97	0.19										
6H-2	52	54	48.690	1.3049	0.512339	±	8	-5.83	0.16										
6H-5	2	4	52.390	1.4732	0.512351	±	8	-5.59	0.17										
6H-6	52	54	54.680	1.5774	0.512292	±	8	-6.76	0.15	0.512291	±	8	-6.77	0.16	0.512181	±	9	-8.91	0.18
7H-3	102	104	61.923	1.8498	0.512365	±	8	-5.32	0.17										
8H-2	52	54	69.536	2.0429	0.512332	±	9	-5.96	0.19										
8H-6	52	54	74.896	2.1788	0.512363	±	12	-5.36	0.23	0.512360	±	8	-5.42	0.15					
9H-2	52	54	78.545	2.2713	0.512350	±	8	-5.62	0.16										
9H-3	103	105	80.825	2.3291	0.512393	±	10	-4.78	0.20										
9H-6	52	54	84.815	2.4303	0.512351	±	9	-5.61	0.18	0.512347	±	8	-5.67	0.16					
10H-1	102	104	86.887	2.4828	0.512385	±	9	-4.93	0.18										
10H-CC	0	3	95.512	2.7506	0.512379	±	7	-5.05	0.15	0.512373	±	8	-5.23	0.16	0.512266	±	9	-7.25	0.18
11H-5	3	5	100.713	2.9363	0.512385	±	7	-4.93	0.13										
12H-1	2	4	105.285	3.0995	0.512374	±	11	-5.14	0.23										
12H-2	53	55	107.295	3.1713	0.512376	±	24	-5.12	0.48	0.512374	±	11	-5.14	0.22					
12H-3	98	100	109.245	3.2409	0.512361	±	10	-5.41	0.20										
13X-3	53	55	113.341	3.3872	0.512398	±	18	-4.68	0.36										
13X-5	52	54	116.331	3.4939	0.512396	±	11	-4.71	0.23										
13X-7	52	54	119.331	3.6010	0.512376	±	7	-5.10	0.14	0.512343	±	9	-5.76	0.18					
14H-3	52	54	123.449	3.7480	0.512401	±	8	-4.63	0.16										
14H-3	94	100	123.889	3.7637	0.512368	±	9	-5.26	0.18	0.512373	±	8	-5.18	0.15					

14H-CC	0	3	124.624	3.7900	0.512407	±	10	-4.51	0.20	0.512383	±	8	-4.97	0.17	0.512281	±	8	-6.96	0.16
15H-3	52	54	127.311	3.8859	0.512354	±	9	-5.54	0.17	0.512370	±	11	-5.23	0.23					
15H-5	52	54	130.311	3.9930	0.512349	±	7	-5.64	0.15										
15H-7	52	54	133.311	4.0838						0.512374	±	8	-5.16	0.16					
16H-CC	0	3	144.128	4.3447						0.512361	±	8	-5.41	0.16	0.512254	±	8	-7.49	0.16
18H-1	52	54	146.456	4.4008	0.512379	±	14	-5.05	0.28	0.512358	±	8	-5.46	0.16	0.512256	±	9	-7.44	0.18
18H-3	52	54	149.456	4.4731						0.512405	±	9	-4.54	0.18	0.512260	±	9	-7.37	0.18
18H-5	52	54	152.456	4.5455						0.512441	±	10	-3.84	0.21	0.512302	±	8	-6.55	0.16
18H-7	52	54	155.456	4.6178						0.512414	±	8	-4.37	0.16	0.512286	±	9	-6.87	0.18
19H-1	52	54	157.281	4.6618						0.512437	±	9	-3.92	0.17	0.512275	±	8	-7.07	0.16
19H-3	52	54	160.281	4.7342	0.512463	±	20	-3.42	0.41										
19H-5	52	54	163.281	4.8065	0.512410	±	14	-4.44	0.28										
20H-1	52	54	167.074	4.8979	0.512413	±	9	-4.40	0.17										
20H-3	52	54	170.074	4.9703	0.512443	±	14	-3.80	0.28	0.512419	±	9	-4.28	0.18	0.512311	±	10	-6.37	0.20
21H-CC	0	3	184.338	5.3142	0.512436	±	19	-3.95	0.37	0.512428	±	9	-4.09	0.18	0.512315	±	8	-6.30	0.16
22H-5	53	55	192.931	5.5214						0.512432	±	10	-4.02	0.21					
23H-5	52	54	202.267	5.7465						0.512433	±	7	-4.00	0.15					
24H-CC	0	3	215.503	6.0657	0.512429	±	19	-4.07	0.38										
25H-1	52	54	216.803	6.0970	0.512448	±	8	-3.70	0.17	0.512434	±	10	-3.98	0.20	0.512349	±	8	-5.63	0.16
26X-5	52	54	227.559	6.4940	0.512417	±	12	-4.31	0.24										
26X-7	52	54	230.359	6.6065	0.512399	±	13	-4.65	0.25										
28H-CC	0	3	241.994	6.9967	0.512413	±	8	-4.40	0.16	0.512428	±	7	-4.11	0.14	0.512328	±	9	-6.04	0.18

		31H-1	52	54	258.862	7.4345	0.512412	±	51	-4.08	0.29										
		31H-5	2	4	264.362	7.6600	0.512407	±	13	-4.51	0.26										
		33H-CC	0	3	283.139	8.4296	0.512405	±	8	-4.55	0.16	0.512407	±	7	-4.50	0.14	0.512326	±	8	-6.08	0.16
		36H-CC	0	3	295.885	8.6384	0.512442	±	8	-3.83	0.17	0.512430	±	9	-4.05	0.17					
		39H-1	52	54	309.963	8.8150	0.512426	±	11	-4.13	0.21	0.512420	±	7	-4.25	0.14					
		40H-CC	0	3	320.698	8.9497	0.512433	±	7	-3.99	0.14	0.512430	±	8	-4.05	0.16	0.512319	±	9	-6.22	0.18
		42H-CC	0	3	329.894	9.0650	0.512440	±	8	-3.85	0.15										
		43H-CC	0	3	338.821	9.2039	0.512437	±	9	-3.92	0.17										
		45H-1	52	54	345.630	9.3191	0.512454	±	9	-3.60	0.17	0.512442	±	8	-3.83	0.16					
		46H-CC	0	3	354.555	9.4701	0.512462	±	12	-3.44	0.24										
		47H-CC	0	3	359.265	9.5497	0.512448	±	8	-3.71	0.17	0.512450	±	8	-3.66	0.15					
		50H-3	52	54	369.430	9.7217	0.512472	±	9	-3.25	0.18	0.512466	±	9	-3.35	0.18	0.512307	±	8	-6.46	0.16
					(CSF-A, m)		**FT/FD**														
DSDP Leg 127	**296**	1R-1 W	65	67	0.66	0.0248	0.512412926	±	9	-4.39	0.17										
		2R-2 W	62	64	8.63	0.3248	0.5124194	±	10	-4.26	0.20										
		3R-1 W	47	49	16.48	0.6203	0.51245574	±	12	-3.56	0.24										
		4R-4 W	55	57	30.56	1.1503	0.51242497	±	4	-4.16	0.16										
		5R-3 W	55	57	38.56	1.4515	0.51243453	±	8	-3.97	0.16										
		6R-5 W	50	52	51.01	1.9201	0.51244158	±	7	-3.83	0.14										
		7R-5 W	50	52	60.51	2.2777	0.512433756	±	11	-3.98	0.22										
		8R-4 W	45	47	68.46	2.5769	0.5124068	±	5	-4.51	0.18										

9R-3 W	50	52	76.51	2.7228	0.512447371	±	12	-3.72	0.24
9R-6 W	43	45	80.94	2.8022	0.512450754	±	10	-3.65	0.20
10R-5 W	63	65	89.14	2.9492	0.51244712	±	14	-3.72	0.28
11R-4 W	63	65	97.14	3.0925	0.512439374	±	8	-3.87	0.15
12R-1 W	105	107	102.56	3.1897	0.51243695	±	15	-3.92	0.30
13R-1 W	123	125	112.24	3.3840	0.512424722	±	8	-4.16	0.17
13R-4 W	82	84	116.33	3.5733	0.512403879	±	9	-4.57	0.17
14R-6 W	74	76	128.75	4.1481	0.512413792	±	8	-4.37	0.16
15R-4 W	63	65	135.14	4.4438	0.512403497	±	8	-4.57	0.17
16R-4 W	56	58	144.57	4.8802	0.5124019	±	7	-4.61	0.14
16R-6 W	77	79	147.78	5.0288	0.512412904	±	9	-4.39	0.18
17R-5 W	92	94	155.93	5.4060	0.512406519	±	13	-4.52	0.26
18R-2 W	60	62	160.61	5.7937	0.512400246	±	10	-4.64	0.19
19R-3 W	64	66	171.65	7.0288	0.512400167	±	9	-4.64	0.19
19R-6 W	56	58	176.07	7.5232	0.51240134	±	8	-4.62	0.16
20R-4 W	82	84	182.83	8.2795	0.51238235	±	8	-4.99	0.16
21R-3 W	64	66	190.65	9.1543	0.512393253	±	9	-4.77	0.18
22R-3 W	68	70	200.19	9.9068	0.512407175	±	8	-4.50	0.15

TABLE DR4. Nd ISOTOPIC COMPOSITIONS OF SEAWATER IN THE JAPAN SEA. THE SURFACE DATA ARE FROM AMAKAWA ET AL. (2004a).

Cruise	Site	Water depth (m)	$^{143}Nd/^{144}Nd$	±	2SE		ε_{Nd}	2SE
KH-98-3	CM-19	0	0.512269	±	0.000008	8	-7.20	0.16
		61	0.512261	±	0.000017	17	-7.36	0.34
		400	0.512274	±	0.000015	15	-7.10	0.3
		581	0.512273	±	0.000014	14	-7.12	0.28
		793	0.512284	±	0.000013	13	-6.91	0.26
		997	0.512289	±	0.000013	13	-6.80	0.25
		1509	0.512297	±	0.000013	13	-6.66	0.25
		1984	0.512272	±	0.000020	20	-7.13	0.39
		2500	0.512289	±	0.000012	12	-6.80	0.24
		2974	0.512282	±	0.000024	24	-6.95	0.47
		3448	0.512282	±	0.000016	16	-6.94	0.31
		3557	0.512295	±	0.000014	14	-6.70	0.28
	CM-20	5	0.512184	±	0.000011	11	-8.86	0.22
		499	0.512284	±	0.000010	10	-6.90	0.19
		990	0.512292	±	0.000008	8	-6.75	0.15
		1983	0.512305	±	0.000008	8	-6.50	0.15
		2727	0.512306	±	0.000013	13	-6.47	0.26